Trajectory optimization of a hypersonic plane s.t. heat limits

Kurt Chudej[1], Armin Rund[2], Markus Wächter[3]
[1]Lehrstuhl für Ingenieurmathematik, Universität Bayreuth
[2]Institut für Mathematik und Wissenschaftliches Rechnen, Karl-Franzens-Universität Graz
[3]German Institute of Science and Technology, TUM Asia Pte Ltd, Singapore
kurt.chudej@uni-bayreuth.de

Extreme thermal loads appear during ascent and reentry of future hypersonic planes. Besides of the availability of a hypersonic propulsion system also an efficient lightweight thermal protection system is mandatory for the feasibility of the entire mission. We consider a trajectory optimization problem enhanced with a PDE modelling the heat load at the stagnation point of the plane. The thermal protection system heats up depending on the flight path. A maximal thermal load is prescribed, which is mathematically modeled as state constraints. These state constraints couple the PDE to the ODE resulting in a fully coupled system. The thermal protection system is discretized in space into several layers using a finite volume scheme. Considering the problem after semidiscretization as a classical ODE constrained optimal control problem, the orders of the state constraints of the different layers are investigated. It turns out that the order is rising with the number of layers starting from two (for the outer layer). The influence of the state constraints is analyzed in numerical experiments. The numerical results are obtained by a direct solution method.

1 Introduction

The design of new hypersonic airplanes is a difficult task. Flying in the hypersonic flight regime yields considerable aerothermic loads. Therefore innovative lightweight materials and a sophisticated thermal protection system (TPS) are mandatory for the airplane. Budget and weight restrictions for the new hypersonic airplane are directly connected with the design of the TPS. One solution approach is to monitor the aerothermic loads during flights. A further step is to find an optimal trajectory which stays below certain thresholds on the different layers of the TPS. This allows to use a not so demanding TPS. Intensive research in designing hypersonic transportation systems was conducted in the 1990s, see e.g. [1–10], and is currently again intensified.

We consider a specific version of the above described trajectory optimization problem. It is an optimal control problem with ordinary (ODE) and partial differential equations (PDE). In particular, the flight path optimization problem is enhanced with a PDE describing the thermal load at the stagnation point, see e.g. [11, 12, 13]. The problem is fully coupled. On the one hand the position and velocity of the ODE-constraint (equations of motion) enter the heat equation of the thermal load. On the other hand a state constraint on the temperature in the TPS establishes an influcence of the PDE on the optimal flight path. Therefore, we have to solve the full optimal control problem s.t. to the ODE, the PDE and the state constraint.

For the numerical solution at first a finite volume approach is used in order to transform the PDE into a system of ODEs. The resulting ODE-constrained optimal control problem s.t. a state constraint is then discretized into a (finite dimensional) nonlinear optimization problem, see e.g. [14] Chap. 4.5.

The aim of the paper is to describe in a detailed mathematical way the coupling between a complicated but standard trajectory optimization problem with an instationary heat equation together with state constraints. We will enhance the previous mathematical description of [13]. The new contribution of this paper lies especially in the detailed analysis of the order of the state constraints of the different layers of the TPS.

Moreover in the meantime the theory and numerics of optimal control s.t. PDE constraints has matured, see e.g. the books [15, 16, 17]. Nevertheless today only a few results for coupled ODE-PDE constrained optimal control problems are available. A simplified version of the hypersonic airplane – a rocket car – was analyzed in [18, 19, 20, 21]. For the rocket car detailed theoretical (and numerical) investigations are available, in particular about the regularity of the Lagrange multipliers and about the nonlocal effects of the state constraint via the heat equation. We compare these effects with those observed in the numerical solution of the much more challenging model of the hypersonic plane.

The article is organized as follows. In Section 2 the trajectory optimization problem is introduced successively. Emphasis is laid on the inequality constraints, the PDE and its discretization. In Section 3 the state constraints are analyzed and a link to DAE-constrained optimal control problems is established. Section 4 reports on a numerical test case of a minimal fuel flight over a given range. The influence of the heating constraint on the optimal flight path is investigated in a comparative study.

2 Optimal control problem

Optimizing the hypersonic flight while considering the thermal protection system gives rise to a complex optimal control problem. Therefore, we introduce the problem step by step. The model of the hypersonic space vehicle together with the TPS is based on [12], see also [11, 13].

We consider a minimum fuel — resp. maximum final mass — range flight over a spherical rotating Earth in the equator plane with free final time t_f. The trajectory optimization problem is modeled as an optimal control problem using five state variables, the velocity $V\,[\mathrm{m/s}]$, the flight path angle $\gamma\,[-]$, the altitude $H\,[\mathrm{m}]$, the range $\zeta\,[\mathrm{m}]$, and the total mass $m\,[\mathrm{kg}]$. Control variables are the angle of attack $\alpha\,[-]$ and the equivalence ratio Φ_L [-] (needed for the computation of the fuel consumption). Based on wellknown equations of motion for flight mechanics, see e.g. [22], the optimal control problem is given as

$$\max_{\alpha(t),\Phi_\mathrm{L}(t),t_\mathrm{f}} \; m(t_\mathrm{f}) \tag{1}$$

s.t.

$$\begin{aligned}\dot V(t) &= f_1(V,\gamma,H,m;\alpha,\Phi_\mathrm{L}) \\ &= [F(V,H;\alpha,\Phi_\mathrm{L})\cos(\alpha) - D(V,H;\alpha)]/m \\ &\quad + \sin\gamma\Big(\omega_\mathrm{E}^2(r_\mathrm{E}+H) - g(H)\Big),\end{aligned} \tag{2}$$

$$\begin{aligned}\dot\gamma(t) &= f_2(V,\gamma,H,m;\alpha,\Phi_\mathrm{L}) \\ &= [F(V,H;\alpha,\Phi_\mathrm{L})\sin(\alpha) + L(V,H;\alpha)]/(mV) \\ &\quad + \cos\gamma\Big(\tfrac{V}{r_\mathrm{E}+H} + \tfrac{\omega_\mathrm{E}^2(r_\mathrm{E}+H)-g(H)}{V}\Big) + 2\,\omega_\mathrm{E}\,,\end{aligned} \tag{3}$$

$$\dot H(t) = V\sin\gamma, \qquad \dot\zeta(t) = V\cos\gamma, \tag{4}$$

$$\dot m(t) = -\dot m_F(V,H;\alpha,\Phi_\mathrm{L})\,, \tag{5}$$

with the gravitational acceleration $g(H) = g_0 r_\mathrm{E}^2/(r_\mathrm{E}+H)^2\,[\mathrm{m/s^2}]$, the gravitational constant $g_0\,[\mathrm{m/s^2}]$, the radius of the Earth $r_\mathrm{E}\,[\mathrm{m}]$ and the angular velocity of the Earth $\omega_\mathrm{E}\,[\mathrm{rad/s}]$. The expressions for the thrust $F(V,H;\alpha,\Phi_\mathrm{L})\,[\mathrm{N}]$, the drag $D(V,H;\alpha)\,[\mathrm{N}]$, the lift $L(V,H;\alpha)\,[\mathrm{N}]$ and the fuel consumption $\dot m_F(V,H;\alpha,\Phi_\mathrm{L})\,[\mathrm{kg/s}]$ are given in [12, 13].

The control and state variables have to fulfill inequalities motivated by technical reasons and model validity. These inequalities consist of state constraints

$$V > 0\,[\mathrm{m/s}],\; -\pi\,[-] \le \gamma \le \pi\,[-],\; H \ge 500\,[\mathrm{m}], \tag{6}$$

$$10\,000\,[\mathrm{Pa}] \le q(V,H) \le 50\,000\,[\mathrm{Pa}], \tag{7}$$

with the dynamic pressure $q(V,H)$ and mixed constraints

$$0\,[\text{-}] \le n(V,H,m;\alpha) \le 2\,[\text{-}], \tag{8}$$

with the load factor $n{=}L(V,H;\alpha)/(mg_0)$. Further, there are technical restrictions to the controls

$$\begin{aligned}-1.5\pi/180\,[-] \le\; &\alpha \;\le 20\pi/180\,[-], \\ \Phi_{\mathrm{L},\min}(V,H) \;\le\; &\Phi_\mathrm{L} \le \Phi_{\mathrm{L},\max}(V,H).\end{aligned} \tag{9}$$

To find an adequate trajectory boundary conditions are added, especially for the range ζ. The numerical example below is a minimal fuel flight over a given range. Therefore the initial and boundary conditions are set to

$$\begin{aligned}V(0) &= 150\,[\mathrm{m/s}] &&, V(t_\mathrm{f}) = 150\,[\mathrm{m/s}], \\ \gamma(0) &= 0\,[-] &&, \gamma(t_\mathrm{f}) = 0\,[-], \\ H(0) &= 500\,[\mathrm{m}] &&, H(t_\mathrm{f}) = 500\,[\mathrm{m}], \\ \zeta(0) &= 0\,[\mathrm{m}] &&, \zeta(t_\mathrm{f}) = 9\cdot 10^6\,[\mathrm{m}], \\ m(0) &= 244\,000\,[\mathrm{kg}].\end{aligned} \tag{10}$$

Up to now, the trajectory optimization problem constitutes a classical ODE control problem with control and state constraints. In the following, the thermal

protection system is accounted for. The heating is modelled using a nonlinear heat equation. Constraining the maximal temperature finally couples the PDE to the ODE, resulting in a fully coupled ODE-PDE control problem.

In hypersonic flight the heating of the plane is heavily influenced by two layers around the plane, the bow shock, and the boundary layer around the plane, see Fig. 1 and 2. While the atmospheric temperature T_∞ can be directly obtained from the altitude H of the vehicle, the temperature after the bow shock T_1 and the temperature in the boundary layer T_e are solutions to a system of nonlinear equations. Therefore it is necessary to compute all atmospheric variables after the bow shock and inside the boundary layer.

Hypersonic flight causes a substantial heating of the aircraft wall, therefore a sophisticated thermal protection system is needed. The thermal protection system consists of several insulated layers of suitable materials and thicknesses. For simplicity we consider here only the most critical stagnation point. Further thermal models for other important parts of the surface, e.g. near the fuel tank, are described e.g. in [11, 12]. At the stagnation point a $d_{\mathrm{TPS}} = 4 \cdot 10^{-3}$ [m] thick layer of carbon fiber reinforced silicon carbide material C/SiC is assumed. The density of the material is $\rho_{\mathrm{TPS}} = 2,100\,[\mathrm{kg/m^3}]$. The heat conductivity λ_{TPS} and heat capacity $c_{\mathrm{p,TPS}}$ of the material are modeled by temperature dependent polynomials of degree three resp. one.

The temperature $\Theta(t,\vec{x})$ in the thermal protection system is dependent on time t and position $\vec{x} \in \Omega$. Ω represents the spatial neighborhood of the stagnation point. The temperature distribution is modelled with the instationary nonlinear heat equation

$$\rho_{\mathrm{TPS}}\, c_{\mathrm{p,TPS}}(\Theta)\frac{\partial \Theta}{\partial t} = \mathrm{div}[\lambda_{\mathrm{TPS}}(\Theta)\mathrm{grad}\,\Theta]\,, \qquad (11)$$

see [13]. We consider in the following for simplicity only a 1D model at the stagnation point. The 3D coordinate $\vec{x}$ is therefore substituted by the 1D spatial axis x (interior normal of the wall), i.e. $x \in [0, d_{\mathrm{TPS}}]$, see Fig. 2. We complete the parabolic PDE with initial and boundary conditions:

$$\begin{aligned}
&\Theta(0,x) = 300\ [\mathrm{K}], \quad x \in [0, d_{\mathrm{TPS}}]\,,\\
&\tfrac{\partial \Theta}{\partial x}(t,0) = \dot{q}_{\mathrm{aero}}(V(t),H(t),\Theta(t,0))\\
&\quad -\varepsilon\sigma(\Theta(t,0)^4 - T_\infty(H)^4), \quad t>0\,, \qquad (12)\\
&\tfrac{\partial \Theta}{\partial x}(t,d_{\mathrm{TPS}}) = \alpha_{\mathrm{q}}(\Theta(t,d_{\mathrm{TPS}}) - T_{\mathrm{in}})\\
&\quad +\varepsilon\sigma(\Theta(t,d_{\mathrm{TPS}})^4 - T_{\mathrm{in}}^4), \quad t>0\,.
\end{aligned}$$

Therein, ε [-] resp. α_{q} $[\mathrm{J/(m^2 \cdot s \cdot K)}]$ denote the emissivity resp. the heat transfer coefficient between the thermal protection system and the air. Both boundary conditions consider heat conduction and radiation. The heat flux $\dot{q}_{\mathrm{aero}}(V,H,\Theta_1)$ on the outer boundary depends on the atmospheric variables in the boundary layer. The formulas for the heat flux $\dot{q}_{\mathrm{aero}}(V,H,\Theta_1)$ can be found in [12, 13].

With the heat equation we monitor the heat distribution in the stagnation point. Additional state constraints $\Theta(t,x) \le \tilde{\Theta}_{\max}(x)$ are imposed. They are subject to material constraints (or budget constraints and might even allow to use less expensive material).

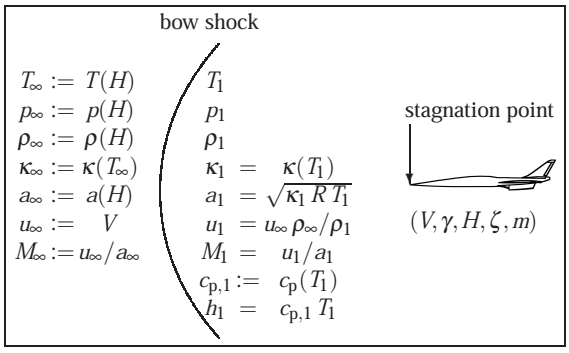

Figure 1: Bow shock in front of airplane (schematic diagram).

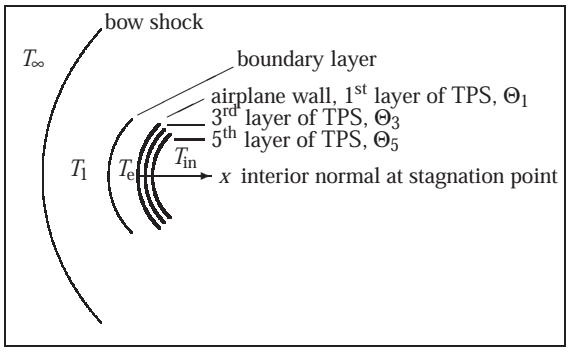

Figure 2: Zoom of Fig. 1, schematic diagram at stagnation point after finite volume discretization.

In the following we apply a semidiscretization. This allows to transform the ODE-PDE optimal control problem to a pure ODE constrained control problem. Accordingly, we can analyze the state constraint using the concept of an order of a state constraint, which is well-established in optimal control s.t. ODEs.

Therefore, we apply a standard finite volume discretization to the different layers of the thermal protection system. In particular, we consider N layers resulting in

$$\begin{aligned}\dot{\Theta}_1(t) &= g_1(\Theta_1,\Theta_2,V,H) = \\ &= [\mathscr{R}_{\text{out}} - \psi_2]/[d\rho_{\text{TPS}}c_{\text{p,TPS}}(\Theta_1)],\end{aligned} \tag{13}$$

$$\begin{aligned}\dot{\Theta}_i(t) &= g_i(\Theta_{i-1},\Theta_i,\Theta_{i+1}) = \\ &= [\psi_i - \psi_{i+1}]/[d\rho_{\text{TPS}}c_{\text{p,TPS}}(\Theta_i)], i = 2,3,N-1,\end{aligned} \tag{14}$$

$$\begin{aligned}\dot{\Theta}_N(t) &= g_N(\Theta_{N-1},\Theta_N) = \\ &= [\psi_N - \mathscr{R}_{\text{in}}]/[d\rho_{\text{TPS}}c_{\text{p,TPS}}(\Theta_N)],\end{aligned} \tag{15}$$

with $\psi_i = \frac{\Theta_{i-1}-\Theta_i}{d}\lambda_{\text{TPS}}\left(\frac{\Theta_{i-1}+\Theta_i}{2}\right)$ and $d = d_{\text{TPS}}/N$ and $T_{\text{in}} = 300\,[\text{K}]$. The boundary conditions of the heat equation are transformed by the discretization to

$$\begin{aligned}\mathscr{R}_{\text{out}} &:= \dot{q}_{\text{aero}}(V,H,\Theta_1) - \varepsilon\sigma\left(\Theta_1^4 - T_\infty(H)^4\right), \\ \mathscr{R}_{\text{in}} &:= \alpha_{\text{q}}\left(\Theta_N - T_{\text{in}}\right) + \varepsilon\sigma\left(\Theta_N^4 - T_{\text{in}}^4\right).\end{aligned} \tag{16}$$

Initial conditions for the temperatures in the layers of the thermal protection system are

$$\Theta_i(0) = 300\ [\text{K}],\ i = 1,\ldots,N. \tag{17}$$

The state constraints transform to

$$\Theta_i(t) \le \Theta_{i,\max},\ i = 1,\ldots,N. \tag{18}$$

3 Analysis of the state contraints

In principle, PDE control problems with additional state constraints are significantly more involved, since the Lagrange multiplier of a pointwise state constraint is a measure only. Therefore, methods that are not formulated in the function space setting normally exhibit mesh dependence, i.e. their iteration count increases with finer meshes. An important aspect for adjoint-based methods is the discretization of the measure. Large errors might occur if it is not resolved properly on the temporal or spatial grid. Also direct methods, even if they are not based on a discretization of the Lagrange multiplier, are usually slower and sometimes might fail to converge. For ODE control problems these difficulties can be analyzed using the order of a state constraint. In the following we will apply this concept for the ODE-PDE control problem after semidiscretization.

For ODE control problems with *scalar* control the order of a state constraint is defined as follows [23]: The expression of a the state constraint is successively differentiated w.r.t. the time while time derivatives of state variables are replaced using the ODE. The order is the minimal number of such differentiation steps until a control variable appears in the expression. It is well-known that the numerical difficulties increase with rising order. It can be explained by linking the problem to a system of differential-algebraic equations (DAE) [24]. In particular, if one considers the active inequalities as equalities, the state-constrained ODE control problem can be interpreted as an optimization problem with a semi-explicit DAE. Accordingly, the differential index of this DAE equals the order of the state constraint increased by one ([25] p. 21, [26]). Consequently, it is well-known that state constraints of order one can be solved accurately, while state constraints of order two lead to instabilities comparable to semi-explicit DAEs of differential index three.

For flight path optimization problems with *multidimensional* controls this has to be generalized to: "a state constraint of order p has differential index $i_{\text{d}} \ge p+1$" [27, 28]. Since the differential index is connected with the perturbation index [29] we also get a glimpse on the numerical difficulties which have to be expected.

In the following we consider the ODE-PDE optimal control problem after semidiscretization in space given by (1–10,13–18). Next we will analyze the order of the state constraints in the context of ODE control.

Theorem: *The dynamic pressure limit (7) is a state constraint of order one. The temperature limit on* Θ_1 *is a state constraint of order two. The temperature limit on* Θ_i *is a state constraint of order* $i+1$, $i = 2,\ldots,N$.

Proof: Since $\dot{q}$ depends explicitely on both controls α and Φ_{L}, the dynamic pressure inequality constraint is a state constraint of order one. On the other hand $\dot{\Theta}_1 = g_1(\Theta_1,\Theta_2,V,H)$ does not contain any control explicitely. We have to differentiate it with respect to time. Obviously $\ddot{\Theta}_1 = \frac{\partial g_1}{\partial V}\dot{V} +$

$\cdots = \frac{\partial g_1}{\partial V} f_1(V,\gamma,H,m;\alpha,\Phi_L) + \phi(V,\gamma,H,m)$ depends on the controls α and Φ_L. Note that in general $\frac{\partial g_1}{\partial V} \neq 0$. Therefore the temperature inequality constraint $\Theta_1 \leq \Theta_{1,\max}$ is a state constraint of order two. Analogous reasoning using (13) proves the rest. We skip the other state constraints (6), since they are not active in the numerical studies below.

The Theorem shows that if the state constraint on the inner layers Θ_i, $i \geq 2$ are not active at all at the optimal solution, then only state constraints of order one or two play a role. This is the case if the maximum of the temperature is always attained at the outer boundary (at the place of the heat source). The numerical results below show this behavior. A proof of such a statement was obtained for a simpler setting in [20] Thm 4.12. Therefore the differential index of the semi-explicit DAE is $i_d \geq 3$, which has already severe numerical consequences.

4 Results

In the following we solve the trajectory optimization problem with $N = 5$ layers and temperature constraints $\Theta_{i,\max} = 1010$, $i = 1,\ldots,N$. The main focus is on the influence of the temperature constraint on the solution. Therefore, the solution is compared to the solution for $\Theta_{i,\max} = \infty$, which will be called the "unconstrained problem" despite the fact that the other inequality constraints (6-10) are included in both cases. In the unconstrained case the heat equation decouples and can be simulated after the optimization. In contrast, an active temperature constraint leads to a fully coupled ODE-PDE control problem.

The presented numerical results are based on a revised Fortran code [13] and were computed using the direct collocation software DIRCOL [30] for the solution of the ODE constrained optimal control problem. The resulting nonlinear program was solved by the SQP-solver SNOPT [31].

The constrained solution exhibits an active temperature constraint $\Theta_1 = \Theta_{1,\max}$ on $t \in [t_{on}, t_{off}]$ with $t_{on} \doteq 1390.57$ [s], $t_{off} \doteq 4866.99$ [s]. Fig. 4 shows the optimized velocities of the constrained and unconstrained case. At the beginning both curves coincide. At around $t \approx 1000$ [s] the velocity is reduced in order to fulfill the temperature constraint later at t_{on}. From this we infer that the state constraint on the PDE has a non-local time effect on the ODE control variables. This is typical for ODE-PDE control problems, and it is in coherence with the observations in the rocket car problem [18, 19, 20, 21]. During the active arc $[t_{on}, t_{off}]$ the velocity is not exactly constant but slightly increasing. Since the velocity in the constrained case is reduced for a long time, the total flight time t_f is increased to meet the boundary condition on the range. The optimal altitude is displayed in Fig. 4. It is slightly increasing during the active arc.

The temperature constraint causes an increase of 6 % in the total flight time, see Tab. 1. While the fuel consumption per time interval is lower due to the lower velocity, the total fuel consumption $m(0) - m(t_f)$ is higher due to the longer flight time t_f. Ascent and descent are rather similar in both cases, but descent starts about 400 [s] later in the constrained case, see Fig. 4.

The controls angle of attack α and equivalence ratio Φ_L are depicted in Fig. 4.

The difference between the unconstrained and the constrained case is mainly because of the active state constraint on the outer layer of the TPS, see Fig. 3. Depicted are the temperatures Θ_i in the i-th layer of the thermal protection system for the reference case and the constrained case. In particular, Θ_1 is active for a long arc $[t_{on}, t_{off}]$. The transition at t_{on} into $\Theta_1 = \Theta_{i,\max}$ for $t \in [t_{on}, t_{off}]$ is smooth, see the zoom in Fig. 3. For the prototype problem of the rocket car, this transition was proven to be differentiable in [21] Thm. 3.3.4. The temperatures in the other layers are nearly constant on approximately the same time interval $[t_{on}, t_{off}]$. They fastly approximate a constant value, their stationary values for $\Theta_1 = \Theta_{\max}$. Due to $T_{in} \ll \Theta_{\max}$, these stationary values drop monotonously in

optimal control problem	**unconstrained** (1–10,13–17)	**constrained** (1–10,13–18)
flight time t_f	6 961.5 [s]	7 378.78 [s]
min. total fuel consumption $m(0) - m(t_f)$	62 486.6 [kg]	62 787.7 [kg]
maximum temperature in TPS: Θ_1	1 124.0 [K]	1 010.0 [K]

Table 1: Results of optimal control

direction to the interior of the plane. Consequently, we observe that the state constraints of order three or more are not active at the optimum.

Alltogether we observe just an active arc (a boundary arc) for one layer. In the continuous description this corresponds to a line $[t_{\text{on}}, t_{\text{off}}] \times x_0$ in the space-time cylinder of the heat equation with $x_0 = 0$. In the case of the rocket car problem there is a full analysis for such active sets and the corresponding line measure, see [21]. In that case, it was proven that the solution to the adjoint PDE is just unbounded at (t_{on}, x_0) and (t_{off}, x_0) and possesses high regularity elsewhere. Consequently, for precise numerical results one specifically has to resolve these locations accurately. Since $x_0 = 0$ is given here, it suffices to resolve the times $t_{\text{on}}, t_{\text{off}}$ accurately via using a fine time grid.

5 Conclusion and Outlook

A complete mathematical description of the coupling of the heat equations including the boundary conditions of the TPS together with the standard trajectory optimization problem is now available. This allows a more detailed mathematical investigation of the (numerical) solution properties. In particular, its semi-discretized version – considered as an ODE-constrained optimal control problem – can be analyzed using the concept of an order of a state constraint. It turns out that the arising state constraints show orders of one or upto $N+1$ for N layers in the TPS. However, the numerical results show that only two state-constraints of order one and two are active, the dynamic pressure limit and the limit on the outer wall temperature Θ_1. These two state constraints already yield an involved optimal control problem. The proposed direct solution method is, however, able to produce the optimal solution.

Since it is out of scope to establish deep theoretical aspects for such a complicated and nonlinear dynamical system describing the hypersonic plane, a simpler prototype problem was set up in former works, the hypersonic rocket car [18, 19, 20, 21]. However, the numerical results for the hypersonic plane are in agreement with the facts that were proven for the rocket car. In particular, the state constraint on the PDE variable is active only on a line in the space time cylinder.

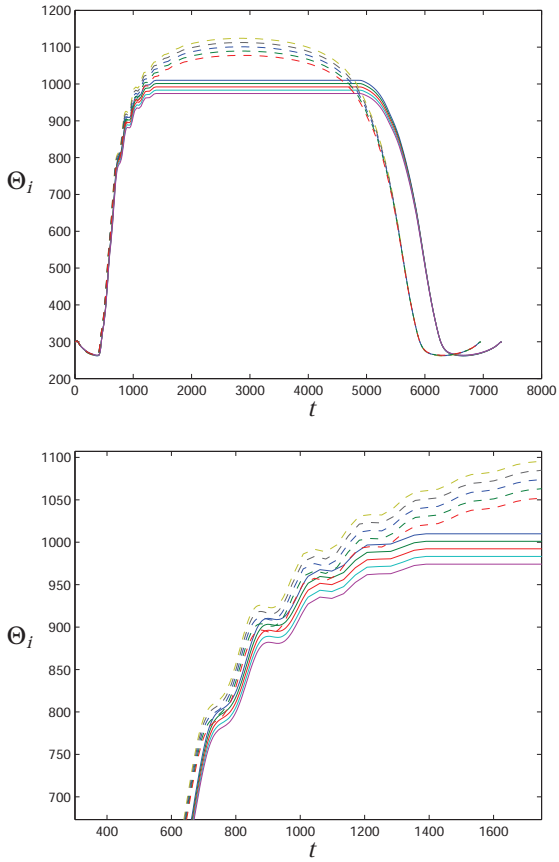

Figure 3: Temperatures Θ_i [K] in the i-th layer of the TPS ($i = 1, \ldots, 5$ from top to bottom) (solid line: constrained, dashed line: unconstrained) and zoom around t_{on}.

This is typical for ODE-PDE control problems, where the controls enter just the ODE. Moreover, the spatial position of the active set is fixed also for the hypersonic plane. Accordingly, the state constraint can be reduced to this spatial position, which frees computational effort and memory for the solution method. Additionally, this reduction might also speed up the convergence of the optimizer.

Coupled ODE-PDE control problems with state constraints, as the one investigated here, frequently arise in applications. However, their analytical and numerical treatment deserves a closer investigation in the future.

References

[1] Högenauer, E.: Raumtransporter. *Zeitschrift für Flugwissenschaften und Weltraumforschung*, 11, pp. 309–316, 1987.

[2] Kuczera, H., Krammer, P., Sacher, P.: *Sänger and the German Hypersonics Technology Programme – Status Report 1991.* 42nd IAF-Congress, Montreal, Canada, Paper-No. IAF-91-198, 1991.

[3] Buhl, W., Ebert, K., Herbst, H.: *Optimal Ascent Trajectories for Advanced Launch Vehicles.* 4th AIAA International Aerospace Planes Conference, Orlando, 1992.

[4] Bayer, R., Sachs, G.: Optimal Return-to-Base Cruise of Hypersonic Carrier Vehicles. *Zeitschrift für Flugwissenschaften und Weltraumforschung*, 19, pp. 47–54, 1995.

[5] Sachs, G., Dinkelmann, M.: Reduction of Coolant Fuel Losses in Hypersonic Flight by Optimal Trajectory Control. *J. Guid. Control Dynam.*, 19, pp. 1278–1284, 1996.

[6] Miele, A., Mancus, S.: Optimal Ascent Trajectories and Feasibility of Next-Generation Orbital Spacecraft. *J. Optimi. Theory App.*, 95, pp. 467–499, 1997.

[7] Windhorst, R., Ardema, M.D., Bowlles, J.V.: *Minimum Heating Reeentry Trajectories for Advanced Hypersonic Launch Vehicles.* Proc. AIAA Guidance, Navigation, and Control Conference, New Orleans, USA, AIAA-97-3535, 1997.

[8] Meese, E., Norstrud, H.: Simulation of Convective Heat Flux and Heat Penetration for a Spacecraft at Re-entry. *Aerosp. Sci. and Technol.*, 6, pp. 185–194, 2002.

[9] Bertin, J.J., Cummings, R.M.: Fifty years of hypersonics: where we've been, where we're going. *Progress in Aerospace Sciences*, 39, pp. 511–536, 2003.

[10] DFG, Deutsche Forschungsgemeinschaft: *Basic Research and Technologies for Two-Stage-to-Orbit Vehicles.* Wiley-VCH Verlag, Weinheim, 2005.

[11] Dinkelmann, M., Wächter, M., Sachs, G.: Modelling and simulation of unsteady heat transfer effects on trajectory optimization of aerospace vehicles. *Mathematics and Computers in Simulation*, 53, pp. 389–394, 2002.

[12] Wächter M.: *Optimalflugbahnen im Hyperschallflug unter Berücksichtigung der instationären Aufheizung*. Dissertation, Lehrstuhl für Flugmechanik und Flugregelung, Technische Universität München, 2004.

[13] Witzgall, M., Chudej, K.: *Flight Path Optimization subject to Instationary Heat Constraints*. In: Troch, I., Breitenecker, F. (eds.): 7th Vienna International Conference on Mathematical Modelling (MATHMOD 2012). - Wien: International Federation of Automatic Control, pp. 1141–1146, 2012.

[14] Betts, J.: *Practical Methods for Optimal Control Using Nonlinear Programming.* SIAM, Philadelphia, 2001.

[15] Tröltzsch, F.: *Optimale Steuerung partieller Differentialgleichungen.* Vieweg+Teubner, Wiesbaden, 2. Auflage, 2009.

[16] Hinze, M., Pinnau, R., Ulbrich, M., Ulbrich, S.: *Optimization with PDE Constraints.* Springer Netherlands, 2009.

[17] Borzi A., Schultz, V.: *Computational Optimization of Systems Governed by Partial Differential Equations.* SIAM, Philadelphia, 2012.

[18] Pesch, H.J., Rund, A., von Wahl, W., Wendl, S.: On Some New Phenomena in State-constrained Optimal Control if ODE as well as PDE are Involved. *Control and Cybernetics*, 39, 3, pp. 647–660, 2010.

[19] Wendl, S., Pesch, H.J., Rund, A.: *On a State-Constrained PDE Optimal Control Problem arising from ODE-PDE Optimal Control*. In: M. Diehl, F. Glineur, and W. Michiels (eds.): Recent Advances in Optimization and its Applications in Engineering. Springer, Heidelberg, pp. 429–438, 2010.

[20] Pesch, H.J., Rund, A., von Wahl, W., Wendl, S.: *On a Prototype Class of ODE-PDE State-constrained Optimal Control Problems. Part 1: Analysis of the State-unconstrained Problems.* Preprint, Universität Bayreuth, 19 pages, 2011; published as appendix C.2 in [21].

[21] Rund, A.: *Beiträge zur Optimalen Steuerung partiell-differential algebraischer Gleichungen.* Dissertation, Fakultät für Mathematik, Physik und Informatik, Universität Bayreuth, 2012.

[22] Miele, A.: *Flight Mechanics. Volume 1: Theory of Flight Paths.* Pergamon Press, 1962.

[23] Hamilton, W.E.: On Nonexistence of Boundary Arcs in Control Problems with Bounded State Variables. *IEEE Trans. Automatic Control*, AC-17, pp. 338–343, 1972.

[24] Eich-Soellner, E., Führer, C.: *Numerical Methods in Multibody Dynamics.* Teubner, Stuttgart, 1998.

[25] Eich, E.: *Projizierende Mehrschrittverfahren zur numerischen Lösung von Bewegungsgleichungen technischer Mehrkörpersysteme mit Zwangsbedingungen und Unstetigkeiten.* VDI Reihe 18, Nr. 109, Düsseldorf, 1992.

[26] Schulz, V.H., Bock, H.G., Steinbach, M.C.: Exploiting Invariants in the Numerical Solution of Multipoint Boundary Value Problems for DAE. *SIAM J. Sci. Comput.*, 19, 2, pp. 440–467, 1998.

[27] Chudej, K., Günther, M.: Global State Space Approach for the Efficient Numerical Solution of State-Constrained Trajectory Optimization Problems. *J. Optimi. Theory App.*, 103, 1, pp. 75–93, 1999.

[28] Chudej, K.: *Effiziente Lösung zustandsbeschränkter Optimalsteuerungsaufgaben.* Habilitation, Fakultät für Mathematik und Physik, Universität Bayreuth, 2001.

[29] Campbell, S.L., Gear, C.W.: The Index of General Nonlinear DAEs. *Numerische Mathematik*, 72, pp. 173–196, 1995.

[30] von Stryk, O.: *Numerische Lösung optimaler Steuerungsprobleme: Diskretisierung, Parameteroptimierung und Berechnung der adjungierten Variablen.* Dissertation, Mathematisches Institut, Technische Universität München, 1994.

[31] Gill, P.E., Murray, W., Saunders, M.A.: SNOPT: An SQP Algorithm for Large-Scale Constrained Optimization. *SIAM Review*, 47, 1, pp. 99–131, 2005.

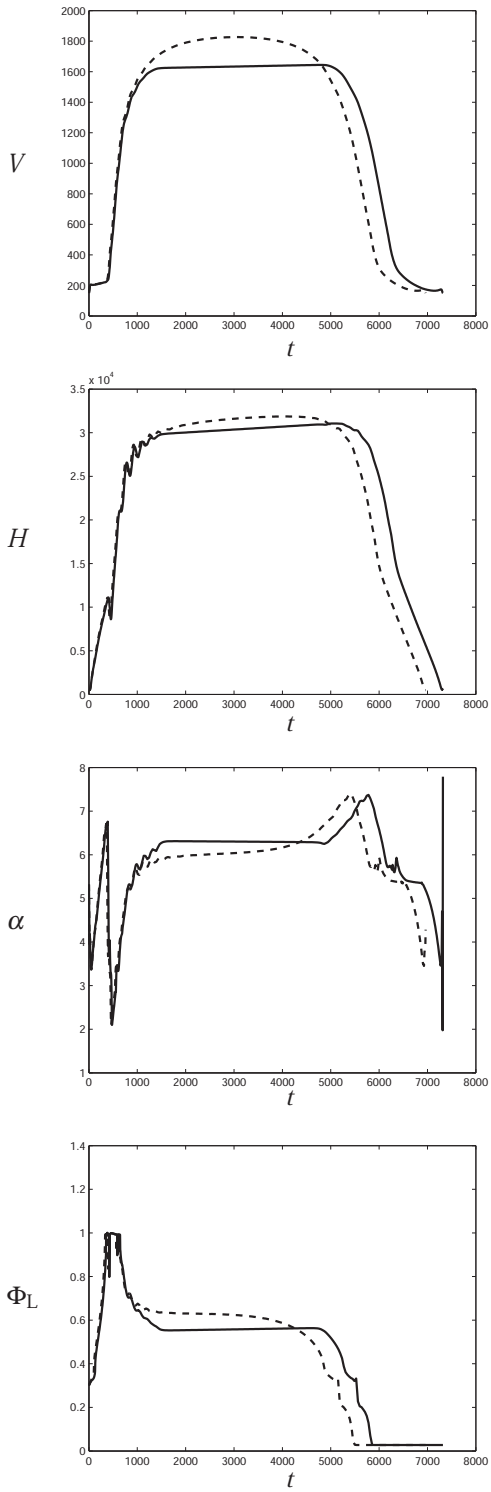

Figure 4: Velocity V [m/s], altitude H [m], angle of attack α, and equivalence ratio Φ_L (solid line: constrained, dashed line: unconstrained)